This article has been accepted for publication in a future issue of this journal, but has not been fully edited. Content may change prior to final publication. Citation information: DOI 10.1109/JIOT.2019.2910875, IEEE Internet of Things Journal

Sustainability Analysis for Fog Nodes with Renewable Energy Supplies

Jiaojiao Jiang, Longxiang Gao, Jiong Jin, Tom H. Luan, Shui Yu, Yong Xiang, and, Saurabh Garg

Abstract—There is a growing interest in the use of renewable energy sources to power fog networks in order to mitigate the detrimental effects of conventional energy production. However, renewable energy sources, such as solar and wind, are by nature unstable in their availability and capacity. The dynamics of energy supply hence impose new challenges for network planning and resource management. In this paper, the sustainable performance of a fog node powered by renewable energy sources is studied. We develop a generic analytical model to study the energy sustainability of fog nodes powered by renewable energy sources, by generalizing the Leaky Bucket model to shape and police traffic source for rate-based congestion control in high-speed fog networks. Based on the closed-form solutions of energy buffer analysis, *i.e.*, the energy depletion probability and mean energy length, we study the energy sustainability in two special but real-happening scenarios. The experimental results show that with proper design the Leaky Bucket model effectively reflects the energy sustainability of data traffic in fog networks. Numerical results also reveal that the model performance is sensitive to certain traffic source characteristics in fog networks.

Index Terms—Fog networks, sustainability analysis, renewable energy

1 Introduction

The explosively growing demand for ubiquitous mobile devices has led to a significant increase in energy consumption by fog networks [1], [2]. To counter this increase, fog networks are expected to make use of renewable energy sources [3], [4], [5], [6], [7], *e.g.*, wind, solar, tides, *etc.*, to fulfill the ever-increasing user demand, while reducing the detrimental effects of conventional energy production [8], [9], [10]. However, unlike traditional energy supplied from the electricity grid, renewable energy sources are often with unstable availability. For example, although solar panels can provide relatively continuous power supply, the energy supply varies across the time of a day and the season of the year, and is influenced by atmospheric conditions and geography. As a result, when renewable energy is deployed to power communication in fog networks, its unreliable nature will affect the availability and efficiency of communications, and therefore will make energy-sustainable network design a necessity.

Many papers have been devoted to address energy consumption issues [11], [12], [13], [14]. For example, in a recent work [11], [15], [16], [17], researchers developed an analytical framework to study the transient evolution of the energy buffer for adaptive resource management and admission control. They model the energy buffer of a fog node as a $G/G/1(/N)$ queuing model [18], [19], [20], which accepts random energy charging process of a general energy arrival pattern (e.g., energy from heterogeneous green energy sources) and general discharging process that fits different mobile applications. These works focus on the goal of maximizing the *network-wide energy sustainability* such that the probability of fog nodes depleting their energy and going out of service is minimized. However, the energy sustainability of *individual fog nodes powered by renewable energy sources* is ignored, especially when processing critical data in *remote rural areas* [21], [22], where keeping individual fog nodes well-functioned in emergency service infrastructures is very crucial. In remote areas such as National Park, emergency communications are essential at any time. It is important for users to connect fog nodes via their own devices, write emergency information (e.g., bush fire), and send it to the administrative department of the park. Hence, it is critical to ensure energy sustainability of individual fog nodes. Meanwhile, the inherent flexibility and high burstiness of data traffic in fog networks, such as transmitting videos and voice, make the shaping and policing of traffic

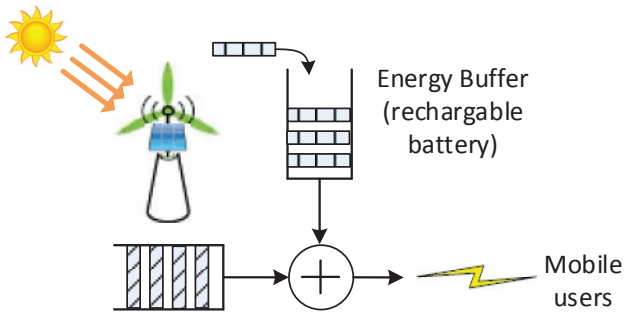

Fig. 1. Structure of a fog node. It consists of an energy buffer charged by solar panels and a data buffer where data are transmitted and consume energy.

- *J. Jiang and J. Jin are with the School of Software and Electrical Engineering, Swinburne University of Technology, Australia (e-mail: jiaojiaojiang@swin.edu.au, jiongjin@swin.edu.au). L. Gao, and Y. Xiang are with the School of Information Technology, Deakin University, Australia (e-mail: longxiang.gao@deakin.edu.au, yong.xiang@deakin.edu.au). T. H. Luan is with the National Key Laboratory of Integrated Networks Services, Xidian University, China (e-mail: tom.luan@xidian.edu.cn). S. Yu is with the School of Software, University of Technology Sydney, Australia (e-mail: shui.yu@uts.edu.au). S. Garg is with the Department of Computing and Information System, Faculty of Engineering and ICT, University of Tasmania, Hobart, TAS, 7001, Australia. (e-mail: Saurabh.Garg@utas.edu.au)*

2327-4662 (c) 2018 IEEE. Personal use is permitted, but republication/redistribution requires IEEE permission. See http://www.ieee.org/publications_standards/publications/rights/index.html for more information.

This article has been accepted for publication in a future issue of this journal, but has not been fully edited. Content may change prior to final publication. Citation information: DOI 10.1109/JIOT.2019.2910875, IEEE Internet of Things Journal

control problems of such networks very critical and make the energy resource management at individual nodes very crucial.

In this paper, we focus on the energy sustainability of fog nodes with renewable energy supplies in fog networks, especially in the remote rural areas. Fig. 1 shows the structure of a fog node charged by solar panels. It is mainly composed of an energy buffer and a data buffer. The energy buffer has variable energy arrival rates due to the unstable availability of renewable energy sources. With adequate energy storage, data traffic in the data buffer could be transmitted and consume energy. We **first** generalize the Leaky Bucket stochastic fluid model [23] to shape and police bursty data traffic in fog networks. In our generalized Leaky Bucket model, we model the incoming data traffic as an N-state Markov modulated fluid sources. The energy arrival rate r reflects different stages of energy supply scenarios. The Leaky Bucket corresponds to a counter, which is incremented each time a cell is generated by the source and is decremented periodically with a suitable leaky rate. The Leaky Bucket can be analyzed as a $G/D/1/N$ queue with finite waiting room N and a suitable arrival process. Each active virtual connection has its own counter. Fig. 2 portrays the Leaky Bucket model on a fog node.

Based on the Leaky Bucket model, we **then** develop a mathematical model to analyze the "*energy sustainability*" performance of fog nodes theoretically under certain energy sustainability constraints. More specifically, we first derive the the closed-form distributions of data buffer and and energy buffer in the stochastic fluid model. Then, we compute the mean lengths of data buffer and energy buffer. According to the mean energy buffer length, we consider two particular but real-happening scenarios of energy sustainability. Again, we use the renewable energy source, solar (see Fig. 1), as an example to introduce the two scenarios. Solar panels can generate relatively stable power energy during sunny daylights, but it cannot generate energy at night. In order to supply ordinary data transmission at night, it is necessary to consider (1) how much data units the remaining energy can supply for ordinary data transmission. Another example would be in raining days, it is reasonable to assume there is no energy supply by solar panel. If the rain last for a few days (in raining season), we need to consider (2) how much remaining energy buffer is required to support a certain days of emergency data transmission. We mathematically analyze energy sustainability related to these two fundamental questions, and finally numerically verify the proposed model can properly reflects energy sustainability of fog nodes.

We summarize the key contributions in this paper as follows.

- We model the high diversity and burstiness of data traffic and energy consumption in fog networks by extending the Leaky Bucket model.
- We derive the the closed-form distributions of data buffer and and energy buffer, and the mean lengths of data buffer and energy buffer.
- According to the Leaky Bucket model, two fundamental questions related to energy sustainability are mathematically analyzed and numerically verified.

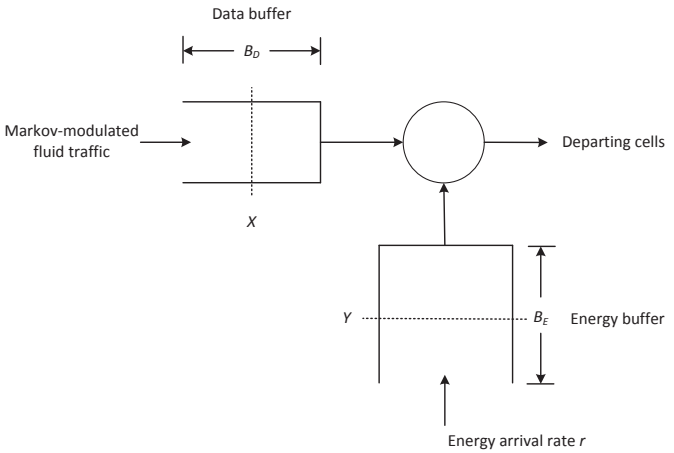

Fig. 2. Leaky Bucket stochastic fluid model. The data traffic is modeled as an *N*-state Markov modulated fluid sources, and the energy supply is modeled with a stage-based constant energy arrival rate.

The rest of this paper is organized as follows. The analysis of the Leaky Bucket model is presented in Section 2. We carry out the analysis of energy sustainability performance in Section 3. Section 4 applies the analysis based on the developed Leaky Bucket model on a simple but illustrative example: the ON-OFF data source scenario. Experimental results of the model performance are presented in Section 5. Section 6 concludes the remarks of this paper.

TABLE 1
Notations used in paper.

Notation	Description
μ_{ij}	The transition rate from state i to state j in the N-state Markov-modulated Poisson process of data flow.
λ_i	The state-dependent rate at state i in the Poisson process.
π_i	The stationary state probability for state i.
B_D	Data bucket capacity in the Leaky Bucket model.
B_E	Energy bucket capacity in the Leaky Bucket model.
X_t	The contents of data buffer at time t.
Y_t	The contents of energy buffer at time t.
α	The transition rate from OFF state to ON state.
β	The transition rate from ON state to OFF state.

2 Modeling Energy Buffering and Data Buffering

In this section, we first introduce a stage-based model for energy buffering. Then, we generalize the Leaky Bucket mechanism to model data traffic shaping and policing at a fog node. The main notations used in this paper are listed in Table 1.

2.1 Stage-based Model of Energy Buffering

With the increasing number of applications moving on to fog networks, using renewable energy to power edge nodes has become a significant strategy to alleviate the increasing

2327-4662 (c) 2018 IEEE. Personal use is permitted, but republication/redistribution requires IEEE permission. See http://www.ieee.org/publications_standards/publications/rights/index.html for more information.

This article has been accepted for publication in a future issue of this journal, but has not been fully edited. Content may change prior to final publication. Citation information: DOI 10.1109/JIOT.2019.2910875, IEEE Internet of Things Journal

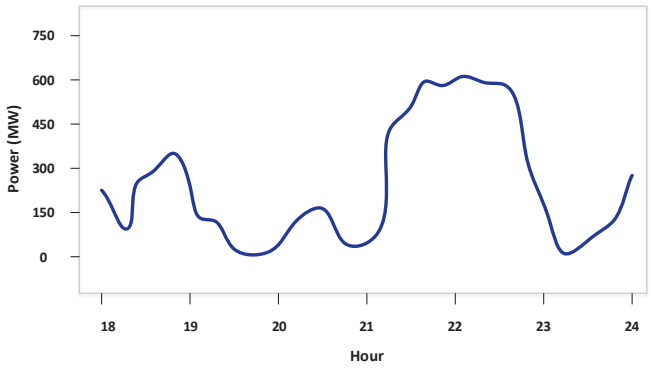

Fig. 3. A typical wind power curve of E.ON Netz in 3rd November 2002 [24].

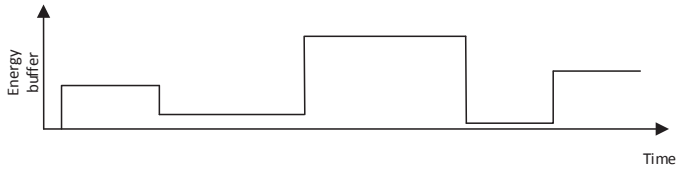

Fig. 4. An illustration of energy buffer at different time stages. It is assumed that the energy power supply keeps consistent within each time stage.

energy demands. In particular, as edge infrastructures are smaller in size than centralized data center, they can make a better use of renewable energy. However, renewable energy source (such as wind power and solar power) is often influenced by atmospheric conditions and geography, so it often presents a fluctuating energy generation process. Figure 3 shows a typical wind power curve of the E.ON Netz area [24] at 3rd November 2002. As we can see it presents a fluctuating process, and it is difficult to mathematically model the dynamic and real-time renewable energy generating process.

In this paper, we simplify the renewable energy generating process by *assuming that renewable energy supply keeps constant at each certain stage* of an hour (or day or week). For example, in Figure 3, it is reasonable to assume that the wind power is relatively in each hour. Another example would be solar energy power. We may split a day into three time stages (7am–10am, 10am–5pm, and 5pm–7am), and solar power output is relatively consistent at each time stage. Fig. 4 illustrates the energy arrival rate differing from stage to stage, but within each stage the energy arrival rate is consistent.

2.2 Leaky Bucket Model of Data Buffering

In this subsection, we generalize the Leaky Bucket mechanism to model data traffic shaping and policing on a fog node. The "Leaky Bucket algorithm" [25], [26], and its performance have been analyzed in many works, such as [27], [28], [29]. Fig. 2 portrays the Leaky Bucket model on a fog node. In general, the Leaky Bucket algorithm is characterized by its bucket depth or threshold (B_D) and its leak rate (B_E) as shown in Fig. 2. The basic idea is that a certain amount of fluid is added to the bucket contents each time a cell enters the network. The bucket leaks at a constant rate set equal to the cell rate as agreed for that particular connection. If cells are sent at a higher rate than the leak rate, the level of the fluid inside the bucket will rise until a certain critical level (the bucket limit) is exceeded. Then it is concluded that the connection violates the agreed rate and the cell is discarded. For discarded cells no fluid is added. All cells for that connection will be blocked until the bucket level has dropped below the limit. Hence, Leaky Bucket algorithm has been commonly used in monitoring peak and average traffic rates of variable bitrate (VBR) services. Through setting the average traffic rates according to the Leaky Bucket algorithm and thereafter we can control traffic. From Fig. 2, we see that there are three critical parameters involved in Leaky Bucket algorithm: energy arrival rate r, energy buffer capacity B_E, and data buffer capacity B_D. Additionally, in the Leaky Bucket model, batteries are required for storing the renewable energy and discharging power in data transmission. Hence, we assume the batteries are with appropriate capacities and a certain number of cycles of useful life. In the following, we will analyze the probabilities of energy buffer and data buffer.

Now, we carry out a general analysis of Leaky Bucket algorithm from which the energy sustainability can be readily derived. Fig. 2 portrays a fluid analysis version of the data traffic. The energy arrival rate and the energy bucket size are r and B_E respectively, and the data buffer size is B_D. The incoming bursty data traffic is modeled as an N-state Markov-modulated Poisson process (MMPP) (see Fig. 5). Transition from state i to state j is governed by a Markov chain with a rate parameter μ_{ij} for $1 \leq i, j \leq N$, and the input rate of the fluid data at state i is λ_i. The underlying continuous time Markov chain of the fluid data for its state transition can be represented by an $N \times N$ infinitesimal generating matrix $\boldsymbol{M}$, defined by

$$\boldsymbol{M} = \begin{bmatrix} \mu_{11} & \mu_{12} & \cdots & \mu_{1j} & \cdots & \mu_{1N} \\ \mu_{21} & \mu_{22} & \cdots & \mu_{2j} & \cdots & \mu_{2N} \\ \vdots & \vdots & & \vdots & & \vdots \\ \mu_{i1} & \mu_{i2} & \cdots & \mu_{ij} & \cdots & \mu_{iN} \\ \vdots & \vdots & & \vdots & & \vdots \\ \mu_{N1} & \mu_{N2} & \cdots & \mu_{Nj} & \cdots & \mu_{NN} \end{bmatrix}, \quad (1)$$

where, the diagonal rate parameter μ_{ii} is given as

$$\mu_{ii} = -\sum_{j=1, j\neq i}^{N} \mu_{ij}, \quad 1 \leq i \leq N. \quad (2)$$

Then, the steady-state probability π_i that the Markov chain is in state i can then be derived by solving the following equation

$$\boldsymbol{\pi M} = 0, \quad (3)$$

where, the row vector $\boldsymbol{\pi}$ is of the N steady state probabilities

$$\boldsymbol{\pi} = \begin{bmatrix} \pi_1 & \pi_2 & \cdots & \pi_i & \cdots & \pi_N \end{bmatrix},$$

and a normalization condition $\sum_{i=1}^{N} \pi_i = 1$.

Assume two random variables X_t and Y_t are the contents of the data buffer and the energy buffer at time t, where $0 \leq X_t \leq B_D$ and $0 \leq Y_t \leq B_E$. The objective is now to find the steady-state occupancy statistics of the two buffers, X_t and Y_t, for the data and energy buffers,

2327-4662 (c) 2018 IEEE. Personal use is permitted, but republication/redistribution requires IEEE permission. See http://www.ieee.org/publications_standards/publications/rights/index.html for more information.

This article has been accepted for publication in a future issue of this journal, but has not been fully edited. Content may change prior to final publication. Citation information: DOI 10.1109/JIOT.2019.2910875, IEEE Internet of Things Journal

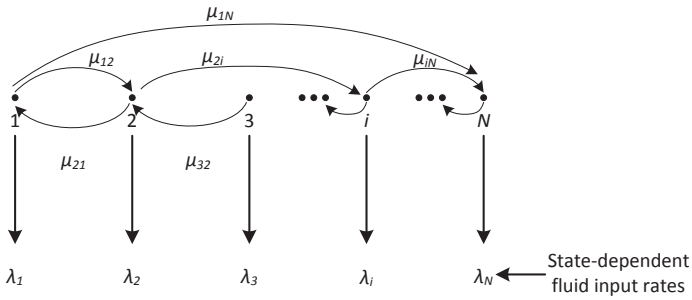

Fig. 5. Markov-modulated fluid data model.

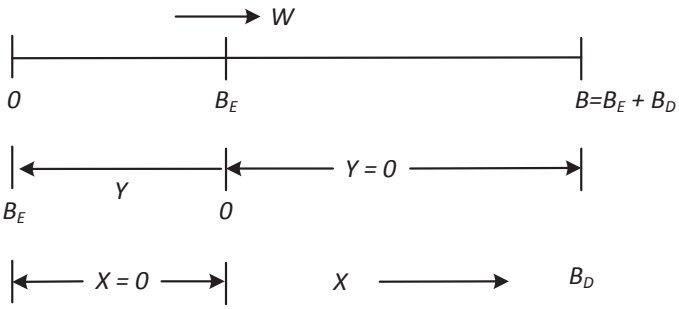

Fig. 6. "Virtual buffer" variable W_t.

respectively. As soon as the buffer occupancy statistics of X_t and Y_t are known, the cell loss and other performance metrics can be found. In practice, however, the statistics of X_t and Y_t cannot be found separately since these two random variables are highly related to each other. Instead, we apply the method in [30], and define an equivalent "virtual" queue representation of X_t and Y_t jointly. Note the following two facts from the Leaky Bucket technique:

1) The data buffer can be occupied only if the energy queue is empty ($Y_t = 0$); otherwise the data cells would be transmitted, one per energy buffer ($X_t \geq 0$). Hence,
$$Y_t = 0,\ X_t \geq 0. \tag{4}$$
2) Conversely, the energy buffer can be occupied only if the data buffer is empty ($X_t = 0$). If data cells were queued, they would each capture a unit of energy and be transmitted ($Y_t \geq 0$). Hence,
$$X_t = 0,\ Y_t \geq 0. \tag{5}$$

The equality ($Y_t = 0, X_t = 0$) in Eq. (4) and Eq. (5) holds for the initial state where data buffer and energy buffer are empty. Now, combining Eqs. (4) and (5), we obtain
$$X_t Y_t = 0. \tag{6}$$

Therefore, instead of finding the individual statistics of X_t or Y_t directly, we shall find the joint probability first from which the data cell loss is then derived.

Following the approach of [30], by combining the two buffers of X_t and Y_t together, we now define the following single "virtual buffer" random variable W_t
$$W_t \equiv X_t - Y_t + B_E. \tag{7}$$

Given the ranges of X_t and Y_t and the condition in Eqs. (4) and (5), by defining B as the sum of the two buffer sizes,
$$B \equiv B_D + B_E. \tag{8}$$

We note that W_t has the following properties:

1) $0 \leq W_t \leq B$.
2) In the range $0 \leq W_t \leq B_E$,
$$X_t = 0,\ W_t = B_E - Y_t. \tag{9}$$
3) In the range $B_E \leq W_t \leq B = B_E + B_D$,
$$Y_t = 0,\ W_t = X_t + B_E. \tag{10}$$

Once the statistics of W_t is found, we can find the statistics of X_t and Y_t using the second and the third property above. The range of W_t and its relation to Y_t are diagrammed in Fig. 6. Define the joint probability of w,
$$F_i(w) = \Pr\left[W_t \leq w,\ S = i\right], \tag{11}$$
at time t at state i of the input data Markov chain, $1 \leq i \leq N$. Note from the definition of W_t that this implies
$$F_i(B) = \pi_i. \tag{12}$$
We derive the solution to $F_i(w)$ based on the approach in [31]. The solution to $F_i(w)$ is given by the solutions to the following set of differential equations,
$$(\lambda_i - r)\frac{F_i(w)}{dw} = \sum_{j=1}^{N} \mu_{ji} F_j(w),\ 1 \leq i \leq N. \tag{13}$$
It is straightforward to obtain the governing differential equations:
$$\frac{d\boldsymbol{F}(w)}{dw}\boldsymbol{D} = \boldsymbol{F}(w)M, \tag{14}$$
where
$$\boldsymbol{F}(w) = \begin{bmatrix} F_1(w) & F_2(w) & \cdots & F_N(w) \end{bmatrix},$$
M is the matrix of Eq. (1), and $\boldsymbol{D}$ is $N \times N$ diagonal matrix
$$\boldsymbol{D} \equiv \text{Diag}\left[\lambda_i - r\right]. \tag{15}$$
Let scalar $F(w)$ be the sum of state probability $F_i(w)$,
$$F(w) = \sum_{i=1}^{N} F_i(w). \tag{16}$$
Combining Eqs. (14) and (16) and the analysis in [32], we obtain the solution to Eq. (14) as follows:
$$d\boldsymbol{F}(w) = \sum_{j=1}^{N} a_j \boldsymbol{\Phi}_j e^{z_j w}, \tag{17}$$
where, $(z_j, \boldsymbol{\Phi}_j)$ is the (eigenvalue, eigenvector) pair satisfying the eigenvalue equation
$$z_j \boldsymbol{\Phi}_j \boldsymbol{D} = \boldsymbol{\Phi}_j \boldsymbol{M},\ 1 \leq j \leq N. \tag{18}$$
The a_j's, $1 \leq j \leq N$, are constants to be determined by invoking N boundary conditions. Since $\boldsymbol{\pi M} = 0$, one eigenvalue of Eq. (18) must be zero. Calling this eigenvalue z_1, its associated eigenvector $\boldsymbol{\Phi}_1 = \boldsymbol{\pi}$. Hence, Eq. (17) can be simplified to
$$\boldsymbol{F}(w) = a_1 \boldsymbol{\pi} + \sum_{j=2}^{N} a_j \boldsymbol{\Phi}_j e^{z_j w}. \tag{19}$$

2327-4662 (c) 2018 IEEE. Personal use is permitted, but republication/redistribution requires IEEE permission. See http://www.ieee.org/publications_standards/publications/rights/index.html for more information.

This article has been accepted for publication in a future issue of this journal, but has not been fully edited. Content may change prior to final publication. Citation information: DOI 10.1109/JIOT.2019.2910875, IEEE Internet of Things Journal

2.3 Distributions of Data Buffer and Energy Buffer

In this subsection, we will derive the closed-form distributions of data and energy buffers based on the Leaky Bucket Model. According to Eq. (19), we know that we need N boundary conditions to find the unknown constants a_j, $1 \leq j \leq N$ to get the explicit form of $\boldsymbol{F}(w)$. To establish these, we note that some of the Markov chain states must be underload or "downward" states for those states i, $\lambda_i < r$; the others must be overload or "upward" states for those States i, $\lambda_i > r$. Hence, all N states of the Markov chain modulating the data arrival rate can be divided into two disjoint sets,

$$S_U \equiv \{i \in N | \lambda_i - r > 0\} : \text{upward states}; \tag{20}$$

and

$$S_D \equiv \{i \in N | \lambda_i - r < 0\} : \text{downward states}. \tag{21}$$

Consider an arbitrary downward state, $i \in S_D$. Since, the data arrival rate is less than the energy arrival rate in these states, $\lambda_i < r$, the energy is tending to collect. The data queue is tending to empty ($X_t \to 0$) and the energy queue is tending to fill ($Y_t \to B_E$). Hence,

$$W_t = X_t - Y_t + B_E \to 0 \tag{22}$$

For these states then, the probability the "virtual queue" is full tends to zero, or we can write

$$\Pr[W_t = B, S = i] = 0, i \in S_D \tag{23}$$

As Eq. (23) is the PDF (Probability Density Function) of W, we note that $\Pr[W_t = B, S = i]$ is equal to the difference between the CDFs (Cumulative Distribution Function) $\Pr[W \leq B, S = i] - \Pr[W_t \leq B^-, S = i]$, *i.e.*, $F_i(B) - F_i(B^-)$. Note that B^- is our notation for the largest value less than B in the PDF of W_t. Given Eq. (12), we thus have

$$F_i(B^-) = \pi_i, \ i \in S_D. \tag{24}$$

Consider an arbitrary upward state, $i \in S_U$. For these states, with $\lambda_i > r$, the energy buffer tends to empty ($Y_t \to 0$), the data buffer tends to fill ($X_t \to B_D$), and

$$W_t = X_t - Y_t + B_E \to B_D + B_E = B. \tag{25}$$

For these states, then, the probability that the virtual queue is empty must be zero. We thus have

$$F_i(0^+) = \Pr[W_t \leq 0^+, S = i] = 0, i \in S_U. \tag{26}$$

Note that 0^+ is our notation for the smallest value larger than 0 in the PDF of W_t.

Since a state is either a downward state or upward state, Eqs. (24) and (26) provide the necessary N boundary conditions from which to find the N unknown constants a_j, $1 \leq j \leq N$, of Eq. (19). The N equations to be solved for the N unknown a_j could be written out in scalar form as follows:

1) $i \in S_D$:

$$F_i(B^-) = \pi_i = a_1 \pi_i + \sum_{j=2}^{N} a_j \Phi_{ji} e^{z_j B^-}. \tag{27}$$

2) $i \in S_U$:

$$F_i(0^+) = 0 = a_1 \pi_i + \sum_{j=2}^{N} a_j \Phi_{ji}. \tag{28}$$

Having found the distributions of W_t, we now can extract from it the distributions of the energy buffer content Y_t and the data buffer content X_t. Specifically, we obtain

$$\Pr[\text{data buffer full}] = 1 - F(B), \tag{29}$$

$$\Pr[\text{energy buffer full}] = F(0), \tag{30}$$

and we also obtain

$$\Pr[X_t \leq x, S = i] = F_i(x + B_E), \ 0 \leq x \leq B_D, \tag{31}$$

and

$$\Pr[Y_t \leq y, S = i] = \pi_i - F_i(B_E - y), \ 0 \leq y \leq B_E, \tag{32}$$

where, $F_i(\cdot)$ and $F(\cdot)$ are defined in Eqs. (11) and (16), respectively.

So far, we have derived the closed-form distributions of data buffer and energy buffer in Eq. (31) and Eq. (32), respectively. Based on these two distributions, we will analyze the energy sustainability in the next section.

3 Energy Sustainability Analysis

Based on the fluid-flow analysis of the Leaky Bucket model, we now study the energy sustainability in this section.

According to the above assumption, we now need to analyze the energy sustainability of fog nodes at certain stage rather. For other stages, we just need to carry out the same analysis on each stage. In the following, we particularly analyze data transmission under some special but real-happening situation—*the fail of energy buffer supply*. Let us consider the solar power energy as an example, where the energy buffer is generated by solar panel. The solar panel can generate relatively stable power energy during sunny daylights. However, it could not generate energy at night. Hence, we need to consider (1) *how much data units the remaining energy can supply for ordinary data transmission*. Particularly, in raining days, it is reasonable to assume there is no energy supply by solar panel. If the rain last for a few days (in raining season), we need to consider (2) *how much remaining energy buffer is required for support a certain days of emergency data transmission*.

In the following sub-sections, we first analyze and derive closed-form distributions of the mean data buffer length and energy buffer length. Then we analyze the energy sustainability under the above two scenarios.

3.1 Mean Data Length and Energy Length

From Eqs. (32) and (31), we can obtain the overall distributions of data buffer and energy buffer [33], [34] as follows:

$$\Pr[X_t \leq x] = \sum_i F_i(x + B_E) = F(x + B_E), \tag{33}$$

and

$$\Pr[Y_t \leq y] = \sum_i (\pi_i - F_i(B_E - y)) = 1 - F(B_E - y). \tag{34}$$

2327-4662 (c) 2018 IEEE. Personal use is permitted, but republication/redistribution requires IEEE permission. See http://www.ieee.org/publications_standards/publications/rights/index.html for more information.

This article has been accepted for publication in a future issue of this journal, but has not been fully edited. Content may change prior to final publication. Citation information: DOI 10.1109/JIOT.2019.2910875, IEEE Internet of Things Journal

Particularly, we have

$$\begin{cases} \Pr[X_t \le B_D] = F(B_D + B_E) = F(B), \\ \Pr[Y_t \le B_E] = 1 - F(B_E - B_E) = 1 - F(0). \end{cases} \tag{35}$$

According to Eq. (19), we obtain the following equation to calculate $F(w)$ for an arbitrary $w \in [0, B]$:

$$F(w) = \sum_i F_i(w) = a_1 + \sum_{j=2}^{N} a_j e^{z_j w} \cdot \sum_i \Phi_{ji} \tag{36}$$

Hence, we can rewrite Eqs. (34) and (33) as follows:

$$\Pr[Y_t \le y] = 1 - \left[a_1 + \sum_{j=2}^{N} a_j e^{z_j (B_E - y)} \cdot \sum_i \Phi_{ji} \right], \tag{37}$$

and

$$\Pr[X_t \le x] = a_1 + \sum_{j=2}^{N} a_j e^{z_j (x + B_E)} \cdot \sum_i \Phi_{ji}. \tag{38}$$

We use $E[X_t]$ to denote the mean data buffer, then $E[X_t]$ can be calculated as follows:

$$\begin{aligned} E[X_t] &= \int_0^{B_D^-} x d\Pr[X_t \le x] + B_D \cdot \Pr[X_t = B_D] \\ &= \int_0^{B_D^-} x d\Pr[X_t \le x] + B_D \cdot (1 - \Pr[X_t < B_D]) \\ &= \int_0^{B_D^-} x d\Pr[X_t \le x] + B_D \cdot (1 - F(B_D + B_E)) \\ &= \int_0^{B_D^-} x d \left[a_1 + \sum_{j=2}^{N} a_j e^{z_j (x + B_E)} \cdot \sum_i \Phi_{ji} \right] \\ &+ B_D \cdot \left(1 - \left[a_1 + \sum_{j=2}^{N} a_j e^{z_j (B_D + B_E)} \cdot \sum_i \Phi_{ji} \right] \right) \\ &= x \left[a_1 + \sum_{j=2}^{N} a_j e^{z_j (x + B_E)} \cdot \sum_i \Phi_{ji} \right] \Bigg|_{x=0}^{x=B_D^-} \\ &- \int_0^{B_D^-} \left[a_1 + \sum_{j=2}^{N} a_j e^{z_j (x + B_E)} \cdot \sum_i \Phi_{ji} \right] dx \\ &+ B_D \cdot \left(1 - \left[a_1 + \sum_{j=2}^{N} a_j e^{z_j (B_D + B_E)} \cdot \sum_i \Phi_{ji} \right] \right) \\ &= (1 - a_1) B_D + \sum_{j=2}^{N} \frac{a_j}{z_j} e^{z_j B_E} \cdot \sum_i \Phi_{ji} \cdot (1 - e^{z_j B_D}). \end{aligned} \tag{39}$$

Similarly, we use $E[Y_t]$ to denote the mean energy buffer, then $E[Y_t]$ can be calculated as follows:

$$\begin{aligned} E[Y_t] &= \int_0^{B_E^-} y d\Pr[Y_t \le y] + B_E \cdot \Pr[Y_t = B_E] \\ &= \int_0^{B_E^-} y d\Pr[Y_t \le y] + B_E \cdot (1 - \Pr[Y_t < B_E]) \\ &= \int_0^{B_E^-} y d\Pr[Y_t \le y] + B_E \cdot F(0) \\ &= \int_0^{B_E^-} y d \left[1 - a_1 - \sum_{j=2}^{N} a_j e^{z_j (B_E - y)} \cdot \sum_i \Phi_{ji} \right] \\ &+ B_E \cdot \left(a_1 + \sum_{j=2}^{N} a_j \cdot \sum_i \Phi_{ji} \right) \\ &= y \left[1 - a_1 - \sum_{j=2}^{N} a_j e^{z_j (B_E - y)} \cdot \sum_i \Phi_{ji} \right] \Bigg|_{y=0}^{y=B_E^-} \\ &- \int_0^{B_E^-} \left[1 - a_1 - \sum_{j=2}^{N} a_j e^{z_j (B_E - y)} \cdot \sum_i \Phi_{ji} \right] dy \\ &+ B_E \cdot \left(a_1 + \sum_{j=2}^{N} a_j \cdot \sum_i \Phi_{ji} \right) \\ &= a_1 B_E - \sum_{j=2}^{N} \frac{a_j}{z_j} \cdot \sum_i \Phi_{ji} \cdot (1 - e^{z_j B_E}). \end{aligned} \tag{40}$$

3.2 Energy Sustainability

Now, suppose there is no energy supply after a certain time. That is to say, the energy arrival rate r becomes 0. Here, we analyze the energy sustainability of the two scenarios described in the opening of Section 3: the maximum data units can be transmitted based on the remaining energy buffer, and the minimum energy buffer required to support a certain period of emergency data transmission. Both of the scenarios requires us to know the upper bound of energy buffer units required for every unit of data transmission. The following analysis investigates the upper bound from the aspect of the average data throughput $\langle \lambda \rangle$.

The average throughput $\langle \lambda \rangle$ can be calculated in a number of equivalent ways. One is to say that this is the average load, other than the cell loss when the data buffer is full. This could be written as

$$\langle \lambda \rangle = \sum_{i=1}^{N} \lambda_i \pi_i - \sum_{i=1}^{N} (\lambda_i - r) \Pr[X_t = B_D, S = i]. \tag{41}$$

The first term on the right-hand side is the average load, averaged over all N states. The second term is the average data cell loss, also averaged over the N states. However, note that the upward states only will be included in the second sum in Eq. (41) since we have already seen that in the downward states the data buffer cannot be full and cells cannot be lost (see Eq. (23)). The probability $\Pr[X_t = B_D, S = i]$ that the data buffer is full with the system in overload state i, is readily calculated as

$$\begin{aligned} &\Pr[X_t = B_D, S = i] \\ &= \Pr[W_t = B, S = i] \\ &= \Pr[W_t \le B, S = i] - \Pr[W_t \le B^-, S = i] \\ &= \pi_i - F_i(B^-). \end{aligned} \tag{42}$$

2327-4662 (c) 2018 IEEE. Personal use is permitted, but republication/redistribution requires IEEE permission. See http://www.ieee.org/publications_standards/publications/rights/index.html for more information.

This article has been accepted for publication in a future issue of this journal, but has not been fully edited. Content may change prior to final publication. Citation information: DOI 10.1109/JIOT.2019.2910875, IEEE Internet of Things Journal

We thus have, from Eq. (41),

$$\langle\lambda\rangle = \sum_{i=1}^{N} \lambda_i \pi_i - \sum_{i=1}^{N} (\lambda_i - r) \left[\pi_i - F_i(B^-)\right]. \quad (43)$$

This can be rewritten as follows,

$$\langle\lambda\rangle = r + \sum_{i=1}^{N} F_i(B^-)(\lambda_i - r). \quad (44)$$

Assuming that every unit of data buffer transmission requires e units energy buffer, then we have the following in-equation

$$e \leq \frac{B_E}{\langle\lambda\rangle}. \quad (45)$$

If $e > B_E/\langle\lambda\rangle$, the arrival energy will aways insufficient for data transmission, which will result into too much data loss in transmission and little energy for sustainability. In addition, energy supply devices generally requires some energy for the basic functionality. Here, we assume an energy supply device needs at least $\xi(\xi \ll B_E)$ energy stored for functionality.

Finally, we analyze energy sustainability for the two aforementioned scenarios. For scenario (1), we need to analyze how much data units the remaining energy can supply for ordinary data transmission. That is to say, the fluid data input rates λ_i are the same as before the fail of energy supply. From Eqs. (39) and (40), we have obtained the mean data buffer left and mean remaining energy buffer. Then, the maximum data units x_{max} the remaining energy can supply is

$$x_{max} = \frac{E[Y_t] - \xi}{e} - E[X_t]. \quad (46)$$

For scenario (2), we need to analyze, how much remaining energy buffer is required to support a certain time of emergency data transmission. That is to say, the average fluid data input rate λ' is different from the average ordinary data input rate λ, where $\lambda \gg \lambda'$. Suppose, over the certain time period (*e.g.*, a day/week/month), the total emergency data is x_{total}. It requires $x_{total} \cdot e$ units of energy to transmit the data. Hence, the minimum energy y_{min} required is

$$y_{min} = (x_{total} + E[X_t]) \cdot e + \xi. \quad (47)$$

Similarly, we can calculate the probability of transmitting x_{total} units of data by adjusting the Leaky Bucket model.

4 Example of ON-OFF Data Sources

In Section 2.2, we model the incoming bursty data traffic as an N-state Markov modulated fluid flow (see Fig. 5), where the transition from state i to state j is governed by a Markov chain with a rate parameter μ_{ij} for $1 \leq i, j \leq N$. In this section, we apply the above proposed Leaky Bucket model and the analysis of energy sustainability on a simple but illustrative 2-state Markov data model, the *ON-OFF data source model* (see Fig. 7). In Fig. 7, the inter-arrival rates are 0 and R_p in the OFF state and the ON state respectively. This could be representative of a voice data source or an image data source, depending on the choice of parameters. Also assume the transition rate from OFF state to ON state is α and from ON state to OFF state is β. In this model, note that the OFF state refers to state 1 and ON state refers to state 2 in the analysis. Notice that $\lambda_1 = 0$, $\lambda_1 = R_p$, and the continuous time Markov chain generating matrix and the steady state probability row vector are as follows

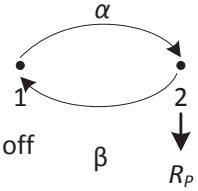

Fig. 7. Simple ON-OFF fluid data source.

$$M = \begin{bmatrix} \mu_{11} & \mu_{12} \\ \mu_{21} & \mu_{22} \end{bmatrix} = \begin{bmatrix} -\alpha & \alpha \\ \beta & -\beta \end{bmatrix},$$

and

$$\boldsymbol{\pi} = \begin{bmatrix} \pi_1 & \pi_2 \end{bmatrix} = \begin{bmatrix} \frac{\beta}{\alpha+\beta} & \frac{\alpha}{\alpha+\beta} \end{bmatrix}.$$

Here, there is only one eigenvalue z to be found. Through basic computation, we have

$$z = -\frac{\alpha+\beta}{R_p - r}(1-\rho), \quad (48)$$

where

$$\rho = \frac{R_p}{r}\left(\frac{\alpha}{\alpha+\beta}\right) = \frac{R_p p}{r}, \text{ with } p \equiv \frac{\alpha}{\alpha+\beta}. \quad (49)$$

For the single eigenvector $\boldsymbol{\Phi} = [\Phi_1, \Phi_2]$ appearing in Eq. (28), we have

$$\Phi_1/\Phi_2 = (R_p - r)/r = \left(\frac{R_p}{r} - 1\right). \quad (50)$$

Letting $\Phi_2 = 1$ arbitrarily, we get, for this example,

$$\boldsymbol{F}(x) = a_1\boldsymbol{\pi} + a_2\left[\left(\frac{R_p}{r} - 1\right), 1\right] e^{zx}. \quad (51)$$

The two unknown constants a_1 and a_2 are found using the boundary conditions of Eqs. (27) and (28). In this simple example, with $N = 2$ states only, state one with $\lambda_1 = 0$ is the downward state and state two with $\lambda_2 = R_p$ is the upward state. We must thus have $0 < r < R_p$ for the fluid analysis to provide a stationary solution in this case. This implies that the single eigenvalue z of Eq. (48) will be negative if the parameter ρ defined by Eq. (49) is less than 1.

From Eq. (27), we have, using Eq. (51),

$$F_1(B^-) = \pi_1 = a_1\pi_1 + a_2\left(\frac{R_p}{r} - 1\right) e^{zB^-}, \quad (52)$$

with $\pi_1 = (1-p) = \beta/(\alpha+\beta)$.

Similarly, from Eqs. (28) and (51), we have

$$F_1(0^+) = 0 = a_1\pi_2 + a_2, \quad (53)$$

where $\pi_2 = p = \alpha/(\alpha+\beta)$.

Solving Eqs. (52) and (53) simultaneously for a_1 and a_2, we get

$$a_1 = 1/\left[1 - \frac{\alpha}{\beta}\left(\frac{R_p}{r} - 1\right) e^{zB}\right], \quad (54)$$

and

$$a_2 = -\pi_2 a_1 = -a_1\alpha/(\alpha+\beta). \quad (55)$$

2327-4662 (c) 2018 IEEE. Personal use is permitted, but republication/redistribution requires IEEE permission. See http://www.ieee.org/publications_standards/publications/rights/index.html for more information.

This article has been accepted for publication in a future issue of this journal, but has not been fully edited. Content may change prior to final publication. Citation information: DOI 10.1109/JIOT.2019.2910875, IEEE Internet of Things Journal

Using Eqs. (54) and (55) in Eq. (51), we finally get the two probability distribution functions in this case of a single ON-OFF data source,

$$F_1(w) = \pi_1 \Delta(w)/\Delta(B), \tag{56}$$

and

$$F_2(w) = \pi_2(1 - e^{zw})/\Delta(B), \tag{57}$$

with

$$\Delta(w) \equiv 1 - \frac{\alpha}{\beta}\left(\frac{R_p}{r} - 1\right)e^{zw}, \tag{58}$$

where $\pi_1 = \beta/(\alpha+\beta)$, $\pi_2 = 1 - \pi_1 = \alpha/(\alpha+\beta)$, and z are given by Eq. (48). Then, we have

$$F(w) = F_1(w) + F_2(w) = \frac{1 - \rho e^{zw}}{\Delta(B)}. \tag{59}$$

All the performance analysis of interest can be obtained from $F(w)$. For example, for the average data throughput, recall that $\lambda_1 = 0$, $\lambda_2 = R_p$, $\rho \equiv R_p p/r$, $p = \alpha/(\alpha+\beta)$ in ON-OFF data sources. Then it is readily shown, using Eqs. (56) and (57) in (44), that the normalized throughput for this example is given by

$$\langle \lambda \rangle / r = 1 - (1-\rho)/\Delta(B), \tag{60}$$

where, $\Delta(B)$ is defined in Eq. (58).

Similarly, the mean length of data buffer $E[X_t]$ in the ON-OFF data sources becomes:

$$\begin{aligned} E[X_t] &= \int_0^{B_D^-} x d[F(x + B_E)] + B_D \cdot (1 - F(B)) \\ &= \int_0^{B_D^-} x d \frac{1 - \rho e^{z(x+B_E)}}{\Delta(B)} + B_D \cdot (1 - \frac{1 - \rho e^{zB}}{\Delta(B)}) \\ &= B_D - \int_0^{B_D^-} d \frac{x - \frac{\rho}{z} e^{z(x+B_E)}}{\Delta(B)} \\ &= B_D - \frac{B_D - \frac{\rho}{z} e^{zB}}{\Delta(B)} + \frac{-\frac{\rho}{z} e^{zB_E}}{\Delta(B)} \\ &= \frac{\rho(e^{zB} - e^{zB_E})}{z\Delta(B)} + B_D(1 - \frac{1}{\Delta(B)}). \end{aligned} \tag{61}$$

The mean length of energy buffer $E[Y_t]$ in ON-OFF data sources becomes:

$$\begin{aligned} E[Y_t] &= \int_0^{B_E^-} y d\left[1 - F(B_E - y)\right] + B_E \cdot F(0) \\ &= \int_0^{B_E^-} y d\left[1 - \frac{1 - \rho e^{z(B_E - y)}}{\Delta(B)}\right] + B_E \cdot \frac{1-\rho}{\Delta(B)} \\ &= B_E - \int_0^{B_E^-} d\left[y - \frac{y + \frac{\rho}{z} e^{z(B_E - y)}}{\Delta(B)}\right] \\ &= \frac{\rho(1 - e^{zB_E})}{z\Delta(B)} + \frac{B_E}{\Delta(B)}. \end{aligned} \tag{62}$$

Then, for the two scenarios of energy sustainability analysis in the ON-OFF data sources, we can get (1) the maximum data buffer x_{max} which could be transmitted when energy rate becomes 0, and (2) the minimum energy buffer y_{min} required for transmitting a certain amount of emergency data transmission.

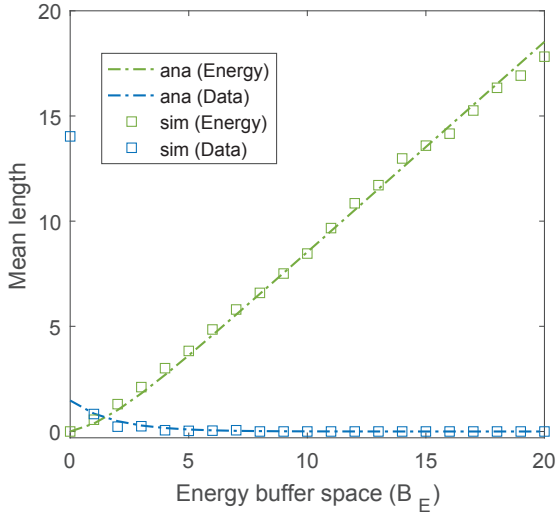

Fig. 8. Mean data length and mean energy length as a function of total buffer space B, with $\rho = 0.81$.

5 Numerical Results

In this section, we validate the energy buffer analysis and evaluate the energy sustainability performance through analytical results and simulation results. All the experiments are implemented on MatLab. We particularly use the ON-OFF data source model for experiments. In the exact Leaky Bucket model, the data source alternates between the ON state and the OFF state. During the ON state, whose mean duration is $1/\beta$ seconds; the source transmits data cells (which are with fixed length packets) at a constant rate of r cells per second. The energy arrives at the energy bucket at a constant rate of r energy buckets per second. To ensure that the data traffic density is relatively moderate (where $\alpha/\beta < 1$) rather than extremely intensive (where $\alpha/\beta \approx 1$), we particularly set β and α to 1.0 and 0.57. We set $R_p = 1$ and r is chosen from $\{0.45, 0.42, 0.39\}$. We set the maximum total buffer size B as 20 and let B_E increase from 0 to 20. For each group of parameter values (in terms of B, B_E and r), we get the average simulation result over 100 runs where each run consists of 100 attempts of data transmission.

We first investigate the mean data length and mean energy length on energy arrival rate (r) and energy buffer size (B_E). From Eqs. (61) and (40), we know that $E[X_t]$ depends on z (which ultimately depends on r), and B_E. The experimental results are shown in Figs. 8, 9, and 10, corresponding to $r = \{0.45, 0.42, 0.39\}$, respectively. From these figures, we see that the the simulation results are very close to the analytical results across different parameter settings. When the energy arrival rate decreases, the simulation results become conservative and thus slightly lower than the analytical results. Overall, the mean energy buffer length increases with the increase of energy buffer size B_E, while the mean data buffer length decreases with the increase of B_E. Moreover, as energy traffic intensity ρ approaches 1 (or alternatively r close to the energy source mean rate), the mean energy buffer length $E[Y_t]$ increases slower with B_E and achieves a desirable as the size of B_E. This is because the greater B_E allows larger data transmission. Hence, the average length of energy becomes larger.

2327-4662 (c) 2018 IEEE. Personal use is permitted, but republication/redistribution requires IEEE permission. See http://www.ieee.org/publications_standards/publications/rights/index.html for more information.

This article has been accepted for publication in a future issue of this journal, but has not been fully edited. Content may change prior to final publication. Citation information: DOI 10.1109/JIOT.2019.2910875, IEEE Internet of Things Journal

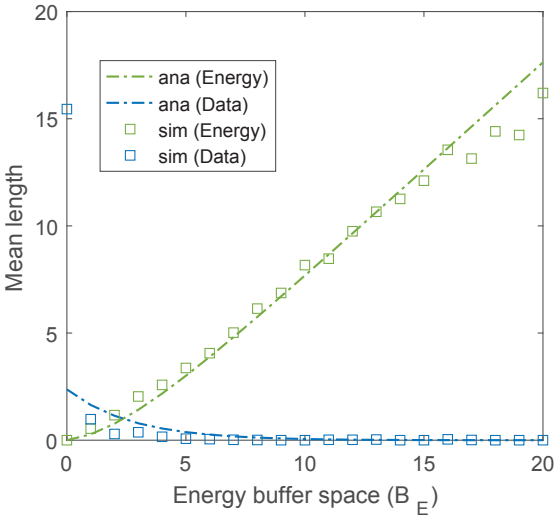

Fig. 9. Mean data length and mean energy length as a function of total buffer space B, with $\rho = 0.87$.

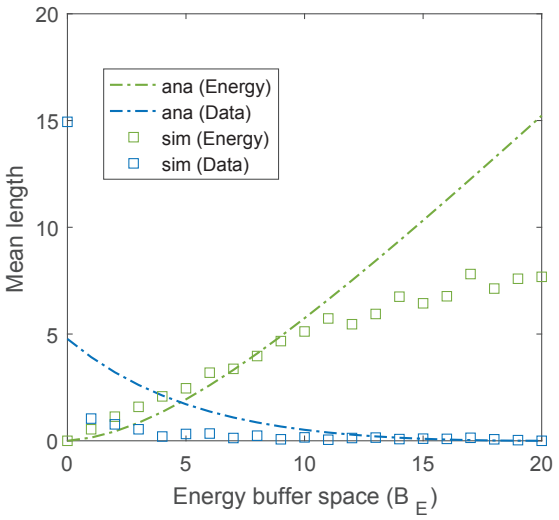

Fig. 10. Mean data length and mean energy length as a function of total buffer space B, with $\rho = 0.93$.

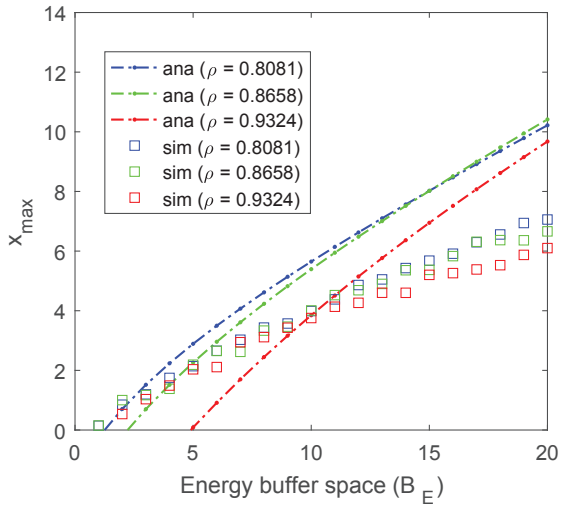

Fig. 11. The maximum units of data that the remaining energy could supply for ordinary data transmission.

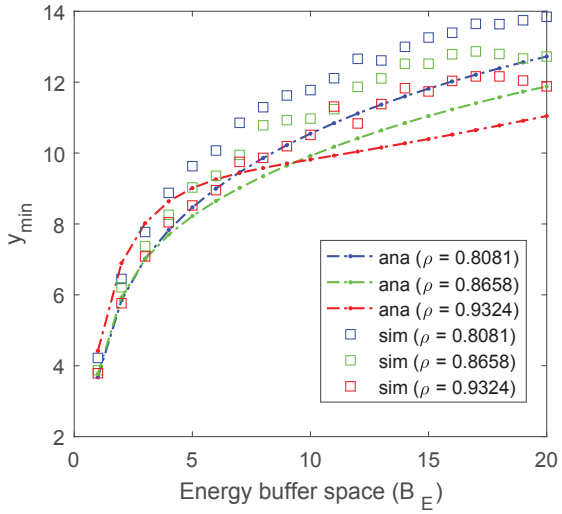

Fig. 12. The minimum units of energy required to support a certain period of emergency data transmission.

We then investigate the energy sustainability of the two particular scenarios discussed in Section 3.2. The results are displayed in Fig. 11 and Fig. 12 for $\rho = \{0.81, 0.87, 0.93\}$ against the energy buffer size B_E. Fig. 11 presents the maximum units x_{max} of data could be transmitted after a failure of energy supply, and Fig. 12 presents the minimum units y_{min} of energy buffer required to supply a certain units of emergency data $d_{emergency}$ transmission. Overall, the simulation results present to be relatively conservative. From the perspective of x_{max}, a smaller number of data units can be transmitted than analytical results when the energy power supply fails. From the perspective of y_{min}, a larger number of energy units are required for emergency data transmission when the energy power supply fails. In Fig. 11, the energy buffer size B_E ranges from 0 to 20 units. As energy buffer size B_E increases, the maximum units x_{max} of data transmission also increases. In particular, the greater ρ (or the less energy arrival rate r) the less data could be transmitted. This is because, the lower energy arrival rate r the less energy can be stored, which in turn support less data transmission after the failure of the energy power supply. In Fig. 12, we particularly set $d_{emergency} = 7$. As we can see, y_{min} increases with B_E. This is because, again, the lower energy arrival rate r the less energy can be stored, which in turn requires much more energy power (y_{min}) for emergency data transmission after the failure of the energy power supply.

6 Conclusion and Discussion

In this paper, we have generalized a stochastic fluid model to analyze the energy sustainability performance on fog nodes. We first generalize the well-known Leaky Bucket model to police and shape traffic from diverse and bursty data sources. Based on the Leaky Bucket model, we derived closed-forms for the distribution of energy buffer and data buffer, and the explicit formulas of mean energy buffer and mean data buffer, and achieved mathematically analysis of the energy sustainability performance on fog nodes. On the

2327-4662 (c) 2018 IEEE. Personal use is permitted, but republication/redistribution requires IEEE permission. See http://www.ieee.org/publications_standards/publications/rights/index.html for more information.

This article has been accepted for publication in a future issue of this journal, but has not been fully edited. Content may change prior to final publication. Citation information: DOI 10.1109/JIOT.2019.2910875, IEEE Internet of Things Journal

basis of the Leaky Bucket model and the derived closed-form formulas, we perform numerical evaluations with the aim of assessing the effectiveness of the Leaky Bucket mechanism and its effectiveness in reflecting the energy sustainability of of data traffic in fog networks. The experimental results have shown how the Leaky Bucket mechanism can be used to police and shape traffic in emergency scenarios (*e.g.*, the failure of energy supply). Numerical results have also revealed the sensitivity of performance to source traffic assumptions.

Note that we assume that the energy arrival rate differs from stage to stage, but within each stage the energy arrival rate is relatively consistent. In the real world, however, the renewable energy sources are often *heterogeneous* [35], and the energy charging process is often *stochastic and may follow certain distribution* (e.g., time-varying Poisson distribution [36]). The Leaky Bucket model generalized in this paper is not applicable for continues time-varying energy charging process. As our future work, we plan to extend the Leaky Bucket model for continues time-varying energy power supply. Meanwhile, in this paper, the data buffer is assumed with no MAC delay and the wireless links are assumed to be reliable. However, real-world data transmission on fog networks often involves MAC delay and unreliable wireless links. Hence, our second future work is to extend current model through considering those realistic network features.

REFERENCES

[1] M. Chiang and T. Zhang, "Fog and iot: An overview of research opportunities," *IEEE Internet of Things Journal*, vol. 3, no. 6, pp. 854–864, 2016.

[2] I. Stojmenovic, S. Wen, X. Huang, and H. Luan, "An overview of fog computing and its security issues," *Concurrency and Computation: Practice and Experience*, vol. 28, no. 10, pp. 2991–3005, 2016.

[3] L. Yu, T. Jiang, Y. Cao, and Q. Qi, "Carbon-aware energy cost minimization for distributed internet data centers in smart microgrids," *IEEE Internet of Things Journal*, vol. 1, no. 3, pp. 255–264, 2014.

[4] H. H. R. Sherazi, G. Piro, L. A. Grieco, and G. Boggia, "When renewable energy meets lora: A feasibility analysis on cable-less deployments," *IEEE Internet of Things Journal*, 2018.

[5] L. Lei, Y. Kuang, X. S. Shen, K. Yang, J. Qiao, and Z. Zhong, "Optimal reliability in energy harvesting industrial wireless sensor networks," *IEEE Transactions on Wireless Communications*, vol. 15, no. 8, pp. 5399–5413, 2016.

[6] Q. Han, B. Yang, C. Chen, and X. Guan, "Energy-aware and qos-aware load balancing for hetnets powered by renewable energy," *Computer Networks*, vol. 94, pp. 250–262, 2016.

[7] T. D. Hieu, B.-S. Kim *et al.*, "Stability-aware geographic routing in energy harvesting wireless sensor networks," *Sensors*, vol. 16, no. 5, p. 696, 2016.

[8] M. Moness and A. M. Moustafa, "A survey of cyber-physical advances and challenges of wind energy conversion systems: prospects for internet of energy," *IEEE Internet of Things Journal*, vol. 3, no. 2, pp. 134–145, 2016.

[9] F. Bonomi, R. Milito, J. Zhu, and S. Addepalli, "Fog computing and its role in the internet of things," in *Proceedings of the first edition of the MCC workshop on Mobile cloud computing*. ACM, 2012, pp. 13–16.

[10] L. M. Vaquero and L. Rodero-Merino, "Finding your way in the fog: Towards a comprehensive definition of fog computing," *ACM SIGCOMM Computer Communication Review*, vol. 44, no. 5, pp. 27–32, 2014.

[11] L. X. Cai, Y. Liu, T. H. Luan, X. Shen, J. W. Mark, and H. V. Poor, "Sustainability analysis and resource management for wireless mesh networks with renewable energy supplies," *IEEE Journal on Selected Areas in Communications*, vol. 32, no. 2, pp. 345–355, 2014.

[12] R. Deng, R. Lu, C. Lai, T. H. Luan, and H. Liang, "Optimal workload allocation in fog-cloud computing toward balanced delay and power consumption," *IEEE Internet of Things Journal*, vol. 3, no. 6, pp. 1171–1181, 2016.

[13] W. Shi, J. Cao, Q. Zhang, Y. Li, and L. Xu, "Edge computing: Vision and challenges," *IEEE Internet of Things Journal*, vol. 3, no. 5, pp. 637–646, 2016.

[14] L. Gao, T. H. Luan, S. Yu, W. Zhou, and B. Liu, "Fogroute: Dtn-based data dissemination model in fog computing," *IEEE Internet of Things Journal*, vol. 4, no. 1, pp. 225–235, 2017.

[15] R. Ranjan, O. Rana, S. Nepal, M. Yousif, P. James, Z. Wen, S. Barr, P. Watson, P. P. Jayaraman, D. Georgakopoulos *et al.*, "The next grand challenges: Integrating the internet of things and data science," *IEEE Cloud Computing*, vol. 5, no. 3, pp. 12–26, 2018.

[16] A. Khoshkbarforoushha, R. Ranjan, R. Gaire, E. Abbasnejad, L. Wang, and A. Y. Zomaya, "Distribution based workload modelling of continuous queries in clouds," *IEEE Transactions on Emerging Topics in Computing*, vol. 5, no. 1, pp. 120–133, 2017.

[17] D. Puthal, S. Nepal, R. Ranjan, and J. Chen, "A dynamic key length based approach for real-time security verification of big sensing data stream," in *International conference on web information systems engineering*. Springer, 2015, pp. 93–108.

[18] J. Kingman, "The single server queue in heavy traffic," in *Mathematical Proceedings of the Cambridge Philosophical Society*, vol. 57, no. 4. Cambridge University Press, 1961, pp. 902–904.

[19] W. Fischer and K. Meier-Hellstern, "The markov-modulated poisson process (mmpp) cookbook," *Performance evaluation*, vol. 18, no. 2, pp. 149–171, 1993.

[20] T. Naishuo, "Queue m/g/1 with adaptive multistage vacation [j]," *Mathematica Applicata*, vol. 4, p. 002, 1992.

[21] J. Li, T. Zhang, J. Jin, Y. Yang, D. Yuan, and L. Gao, "Latency estimation for fog-based internet of things," in *Telecommunication Networks and Applications Conference (ITNAC), 2017 27th International*. IEEE, 2017, pp. 1–6.

[22] T. Khatib, A. Mohamed, and K. Sopian, "A review of photovoltaic systems size optimization techniques," *Renewable and Sustainable Energy Reviews*, vol. 22, pp. 454–465, 2013.

[23] M. P. McGarry, M. Maier, and M. Reisslein, "Ethernet pons: a survey of dynamic bandwidth allocation (dba) algorithms," *IEEE communications magazine*, vol. 42, no. 8, pp. S8–15, 2004.

[24] B. Ernst, K. Rohrig, and R. Jursa, "Online-monitoring and prediction of wind power in german transmission system operation centres," in *Proceedings of the First IEA Joint Action Symposium on Wind Forecasting Techniques, Norrköping, Sweden*, 2002, pp. 125–145.

[25] M. Schwartz, *Broadband integrated networks*. Prentice Hall PTR New Jersey, 1996, vol. 19.

[26] G. Niestegge, "The leaky bucketpolicing method in the atm (asynchronous transfer mode) network," *International Journal of Digital & Analog Communication Systems*, vol. 3, no. 2, pp. 187–197, 1990.

[27] N. Yamanaka, Y. Sato, and K.-I. Sato, "Performance limitation of leaky bucket algorithm for usage parameter control and bandwidth allocation methods," *IEICE Transactions on Communications*, vol. 75, no. 2, pp. 82–86, 1992.

[28] N. Yin and M. G. Hluchyj, "Analysis of the leaky bucket algorithm for on-off data sources," *Journal of High Speed Networks*, vol. 2, no. 1, pp. 81–98, 1993.

[29] K. Sohraby and M. Sidi, "On the performance of bursty and modulated sources subject to leaky bucket rate-based access control schemes," *IEEE Transactions on Communications*, vol. 42, no. 234, pp. 477–487, 1994.

[30] A. I. Elwalid and D. Mitra, "Stochastic fluid models in the analysis of access regulation in high speed networks," in *Global Telecommunications Conference, 1991. GLOBECOM'91.'Countdown to the New Millennium. Featuring a Mini-Theme on: Personal Communications Services*. IEEE, 1991, pp. 1626–1632.

[31] D. Anick, D. Mitra, and M. M. Sondhi, "Stochastic theory of a data-handling system with multiple sources," *Bell Labs Technical Journal*, vol. 61, no. 8, pp. 1871–1894, 1982.

[32] B. Noble, J. W. Daniel *et al.*, *Applied linear algebra*. Prentice-Hall New Jersey, 1988, vol. 3.

[33] B. Everitt and A. Skrondal, *The Cambridge dictionary of statistics*. Cambridge University Press Cambridge, 2002, vol. 106.

[34] G. F. Reed, F. Lynn, and B. D. Meade, "Use of coefficient of variation in assessing variability of quantitative assays," *Clinical and diagnostic laboratory immunology*, vol. 9, no. 6, pp. 1235–1239, 2002.

2327-4662 (c) 2018 IEEE. Personal use is permitted, but republication/redistribution requires IEEE permission. See http://www.ieee.org/publications_standards/publications/rights/index.html for more information.

This article has been accepted for publication in a future issue of this journal, but has not been fully edited. Content may change prior to final publication. Citation information: DOI 10.1109/JIOT.2019.2910875, IEEE Internet of Things Journal

[35] R. Mahmud, R. Kotagiri, and R. Buyya, "Fog computing: A taxonomy, survey and future directions," in *Internet of everything*. Springer, 2018, pp. 103–130.

[36] A. Ihler, J. Hutchins, and P. Smyth, "Adaptive event detection with time-varying poisson processes," in *Proceedings of the 12th ACM SIGKDD international conference on Knowledge discovery and data mining*. ACM, 2006, pp. 207–216.

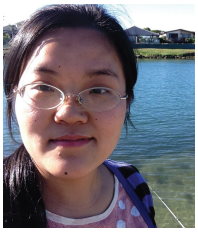

Jiaojiao Jiang received the Ph.D. degree in School of Information Technology from Deakin University, Australia in 2017. She is currently a Postdoctoral Research Fellow in the School of Software and Electrical Engineering, Swinburne University of Technology, Australia. Her research interests include service virtualization, cyber security, and complex networks. She has served as Program Chair, TPC Chair, Symposium Chair, and Session Chair for a number of international conferences, including GlobeCom and ICC.

Longxiang Gao received his PhD in Computer Science from Deakin University, Australia. He is currently a Lecturer at School of Information Technology, Deakin University. Before joined Deakin University, he was a post-doctoral research fellow at IBM Research & Development Australia. His research interests include data processing, mobile social networks, Fog computing and network security. Dr. Gao has over 40 publications, including patent, monograph, book chapter, journal and conference papers. Some of his publications have been published in the top venue, such as IEEE TMC, IEEE IoT, IEEE TDSC and IEEE TVT. Dr. Gao is a Senior Member of IEEE and active in IEEE Communication Society. He has served as the TPC co-chair, publicity co-chair, organization chair and TPC member for many international conferences.

Jiong Jin received the B.E. degree with First Class Honours in Computer Engineering from Nanyang Technological University, Singapore, in 2006, and the Ph.D. degree in Electrical and Electronic Engineering from the University of Melbourne, Australia, in 2011. He is currently a Senior Lecturer in the School of Software and Electrical Engineering, Faculty of Science, Engineering and Technology, Swinburne University of Technology, Melbourne, Australia. Prior to it, he was a Research Fellow in the Department of Electrical and Electronic Engineering at the University of Melbourne from 2011 to 2013. His research interests include network design and optimization, fog and edge computing, robotics and automation, Internet of Things and cyber-physical systems as well as their applications in smart manufacturing and smart cities.

Tom H. Luan received his B.Eng. degree from Xi'an Jiao Tong University, China, in 2004, the M.Phil. degree from Hong Kong University of Science and Technology in 2007, and Ph.D. degree from the University of Waterloo, Ontario, Canada, in 2012. He is a professor at the School of Cyber Engineering of Xidian University, Xi'an, China. His research mainly focuses on content distribution and media streaming in vehicular ad hoc networks and peer-to-peer networking, as well as the protocol design and performance evaluation of wireless cloud computing and edge computing. Dr. Luan has authored/coauthored more than 40 journal papers and 30 technical papers in conference proceedings, and awarded one US patent. He served as a TPC member for IEEE Globecom, ICC, PIMRC and the technical reviewer for multiple IEEE Transactions including TMC, TPDS, TVT, TWC and ITS.

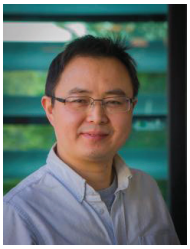

Shui Yu is currently a full Professor of School of Software, University of Technology Sydney, Australia. Dr Yus research interest includes Security and Privacy, Networking, Big Data, and Mathematical Modelling. He has published two monographs and edited two books, more than 200 technical papers, including top journals and top conferences, such as IEEE TPDS, TC, TIFS, TMC, TKDE, TETC, ToN, and INFOCOM. Dr Yu initiated the research field of networking for big data in 2013. His h-index is 32. Dr Yu actively serves his research communities in various roles. He is currently serving the editorial boards of IEEE Communications Surveys and Tutorials, IEEE Communications Magazine, IEEE Internet of Things Journal, IEEE Communications Letters, IEEE Access, and IEEE Transactions on Computational Social Systems.

Yong Xiang received the Ph.D. degree in Electrical and Electronic Engineering from The University of Melbourne, Australia. He is a Professor and the Director of the Artificial Intelligence and Image Processing Research Cluster, School of Information Technology, Deakin University, Australia. His research interests include information security and privacy, signal and image processing, data analytics and machine intelligence, and Internet of Things. He has published 2 monographs, over 100 refereed journal articles, and numerous conference papers in these areas. He is an Associate Editor of IEEE Signal Processing Letters and IEEE Access. He has served as Program Chair, TPC Chair, Symposium Chair, and Session Chair for a number of international conferences.

Saurabh Garg is currently a Lecturer with the University of Tasmania, Australia. He is one of the few Ph.D. students who completed in less than three years from the University of Melbourne. He has authored over 40 papers in highly cited journals and conferences. During his Ph.D., he has been received various special scholarships for his Ph.D. candidature. His research interests include resource management, scheduling, utility and grid computing, Cloud computing, green computing, wireless networks, and ad hoc networks.

2327-4662 (c) 2018 IEEE. Personal use is permitted, but republication/redistribution requires IEEE permission. See http://www.ieee.org/publications_standards/publications/rights/index.html for more information.